Talanta 134 (2015) 132–135

Contents lists available at ScienceDirect

Talanta

journal homepage: www.elsevier.com/locate/talanta

Dual-functional Pt-on-Pd supported on reduced graphene oxide hybrids: Peroxidase-mimic activity and an enhanced electrocatalytic oxidation characteristic

Xiahong Zhang [a], Genghuang Wu [b], Zhixiong Cai [b], Xi Chen [b,*]

[a] Department of Chemical and Material Engineering, Longyan College, Longyan 364000, Fujian, China
[b] Department of Chemistry and the MOE Key Laboratory of Spectrochemical Analysis & Instrumentation, College of Chemistry and Chemical Engineering, State Key Laboratory of Marine Environmental Science, Xiamen University, Xiamen 361005, China

ARTICLE INFO

Article history:
Received 30 July 2014
Received in revised form
30 October 2014
Accepted 1 November 2014
Available online 10 November 2014

Keywords:
Peroxidase-mimic
H_2O_2
PtPd
Reduced graphene oxide
Fuel cell

ABSTRACT

In this study, a facile hydrothermal method was developed to synthesize Pt-on-Pd supported on reduced graphene oxide (Pt-on-Pd/RGO) hybrids. Because of the synergistic effect between Pt-on-Pd and RGO, the obtained Pt-on-Pd/RGO had superior peroxidase-mimic activities in H_2O_2 reduction and TMB oxidation. The reaction medium was optimized and a sensing approach for H_2O_2 was developed with a linear range from 0.98 to 130.7 μM of H_2O_2. In addition, the characteristic of electrocatalytic oxidation of methanol was investigated. The peak current density value, j_f, for the Pt-on-Pd/RGO hybrid (328 mA mg_{Pt}^{-1}) was about 1.85 fold higher than that of commercial Pt black (177 mA mg_{Pt}^{-1}) and, also, more durable electrocatalytic activity could be obtained. For the first time, the dual-functional Pt-on-Pd/RGO with peroxidase-mimic activity and an enhanced electrocatalytic oxidation characteristic was reported.

1. Introduction

Owing to their immense catalytic power and remarkable substrate specificity under mild reaction conditions, enzymes have been attracting interest in pharmaceutical processes, biosensing, and the environmental and food fields [1,2]. However, problems such as low operational stability as well as high cost and time-consuming preparation, purification and storage of natural enzymes largely limit their applications. The emergence and recent advance of nanoscience and nanotechnology provide new opportunities for the application of nanomaterials, and artificial enzyme mimics are a current research interest. Fe_3O_4 has been described with peroxidase-like activity [3] and since then, noble metals such as Pt nanoparticles (PtNPs) [4], Ag based bimetallic alloy nanostructures [5], dumbbell-like PtPd–Fe_3O_4 [6] and PtPd–Au nanorods [7] are also reported with peroxidase-like activity. Recently, one of the most important derivatives of graphene, graphene oxide (GO), a pseudo-two-dimensional carbon material with an oxygen-containing functional group is shown to have intrinsic peroxidase-like activity [8]. Furthermore, the surprisingly high catalytic activity of an Au cluster supported on GO is reported [9], indicating that GO can serve as the enzyme modulator to regulate peroxidase-like activity.

For the noble metal Pt, another remarkable property is its excellent electrocatalytic activity in fuel cells. However, its high cost and low CO poisoning tolerance severely limit the wider adoption of a Pt catalyst [10,11]. To address this problem, carbon supported Pt nanomaterials have been widely used to improve the stability of the catalyst and to reduce the usage of Pt [12,13]. As novel support materials, graphene and GO are proved to enhance the performance of a Pt based catalyst and so indicate a bright future [14]. Meanwhile, Pt-based bimetallic nanomaterial is proposed as a substitute for the fuel cell catalysts, since the incorporation of metal in the nanomaterial alters the surface electronic structure of Pt and subsequently improves its resistance to poisonous substances as well as enhancing its catalytic activity [15]. Recently, in order to combine the characteristics of Pt–Pd alloy and reduced GO (RGO), some method including electrochemical reduction [16] and wet-chemical strategy [17] have been developed to construct PtPd nanostructures supported on an RGO hybrid; however, these methods were not facile or the product surfaces were not clean enough. Based our previous works, PdNPs/GO [18] and PtNPs/RGO [19] are synthesized using a spontaneous redox reaction. In this study, Pt-on-Pd/RGO composites were obtained by modifying the previous reaction conditions [19]. The catalytic activity of the synthesized Pt-on-Pd/RGO was investigated in H_2O_2

* Corresponding author. Tel./fax: +86 592 2184530.
E-mail address: xichen@xmu.edu.cn (X. Chen).

http://dx.doi.org/10.1016/j.talanta.2014.11.002
0039-9140/

reduction and 3,3′,5,5′-tetramethylbenzidine (TMB, peroxidase substrate) oxidation. In order to reveal the potential applications of Pt-on-Pd/RGO in both biosensing and fuel cells, the activity of Pt-on-Pd/RGO was compared with that of commercial Pt black through the study of the electro-catalytic oxidation characteristic of methanol.

2. Experimental section

2.1. Materials

Graphite powder was purchased from the Lvyin Co. (Xiamen, China). $KMnO_4$, H_2SO_4, $NaNO_3$, H_2O_2 and methanol were obtained from the Chemical Reagent Company of Shanghai (China). TMB and Pt black catalyst were purchase from the Aldrich Chem. Co. (USA). K_2PdCl_4 and K_2PtCl_4 were obtained from the Wake Pure Chemicals Co. Ltd. (Osaka, Japan), and rod glassy carbon electrodes (GCEs) were from the BAS Co. Ltd. (Tokyo, Japan). All other reagents were of analytical grade and used without further purification. The pure water for solution preparation was from a Millipore Autopure WR600A system (Millipore Ltd., USA).

2.2. Instruments

The morphology of Pt-on-Pd/RGO was examined using a high resolution transmission electron microscope (HRTEM, FEI Tecnai-F30 FEG). Surface analysis performed using X-ray photoelectron spectroscopy (XPS) was carried out on PHI Quantum-2000 XPS equipment. Absorption spectra were recorded on a Shimadzu UV-2550 UV–vis spectrophotometer. Electrochemical measurements were performed using a CHI 660B Electrochemical Analyzer (CHI Co., Shanghai, China). A conventional three-electrode system was used comprising a GCE coated with Pt-on-Pd/RGO film as the working electrode, a platinum auxiliary electrode and a saturated calomel reference electrode. Before the preparation of the modified GCE, the GCE was polished with 1, 0.3 and 0.05 μm α-Al_2O_3, sequentially. For coating the GCE surface with Pt-on-Pd/RGO nanocomposite, we use Nafion to consolidate the modification. 20 μL of Pt-on-Pd/RGO suspension was dispersed in 20 μL 0.5% Nafion ethanol solution, then deposited 5 μL of Pt-on-Pd/RGO/Nafion on the polished GCE and dried in the air for 4 h at 25 °C.

2.3. Preparation of RGO and Pt-on-Pd/RGO

RGO was synthesized using a KOH medium hydrothermal method based on our previous studies [19]. In a typical experiment, 140.3 mg KOH was added to 50 mL 0.5 mg mL^{-1} GO solution, and kept the final KOH concentration of 50 mM. The solution was heated in an oil bath at 100 °C for 20 h to obtain RGO. For preparation of Pt-on-Pd/RGO, 2 mL RGO was kept at 80 °C, a mixture of 560 μL 10 mM K_2PtCl_4 and 80 μL 10 mM K_2PdCl_4 was added under vigorous stirring. The solution was then kept at 80 °C for 6 h. After reaction, the mixture was centrifuged and washed once with 50 mM H_2SO_4 and four times with pure water to remove the remaining reagents. The sediment was finally redispersed in 0.5 mL H_2O.

2.4. Catalytic oxidation of TMB by Pt-on-Pd/RGO

To investigate the catalytic activity of the as-prepared hybrids, the oxidation reaction of TMB was tested in the presence of H_2O_2. In a standard procedure, 5 μL Pt-on-Pd/RGO was added into 2 mL phosphate buffer saline (PBS, pH 5.2) with different concentrations of H_2O_2 at 30 °C for 10 min. The reaction was carried out in a quartz cuvette.

3. Results and discussion

3.1. Characterization of Pt-on-Pd/RGO

The TEM and HRTEM images depicted in Fig. 1 are direct morphological observations of the Pt-on-Pd/RGO. As shown in Fig. 1a, the characteristic wrinkles on the sheet indicated the edge of the RGO. Nanoscale pores on the surface of the RGO were attributed to the reaction between KOH and GO, resulting in the reduction and a recovery of the conductivity of RGO [20]. In addition, Pt-on-Pd was well dispersed on the RGO with a high density. Several NPs around 3 nm tend to assemble together (Fig. 1b). HRTEM images (Fig. 1c) reveal that several Pt branches had grown from a darker Pd center [21] into a dendritic structure. The diameter of the Pd center (denoted by the white circle) was about 3–6 nm. In addition, several single particles were observed, which could be attributed to the direct reaction between $PtCl_4^{2-}$ and RGO.

3.2. Pt-on-Pd/RGO as a peroxidase mimic and its use in H_2O_2 detection

TMB is generally used as a horseradish peroxidase (HRP) substrate in various bioassays and has been widely used to demonstrate peroxidase-like activity. In a typical TMB oxidation process, the color of the transparent substrate (TMB and buffer solution) turns blue after the addition of catalysts and H_2O_2. In our experiment, UV–vis spectra were employed to evaluate the peroxidase activity of the Pt-on-Pd/RGO. Similar to HRP, the peroxidase activity of the Pt-on-Pd/RGO was greatly dependent on the medium pH. At pH 7.4 PBS, no obvious change of color or UV spectra could be obtained. After optimization, a pH 5.2 PBS was

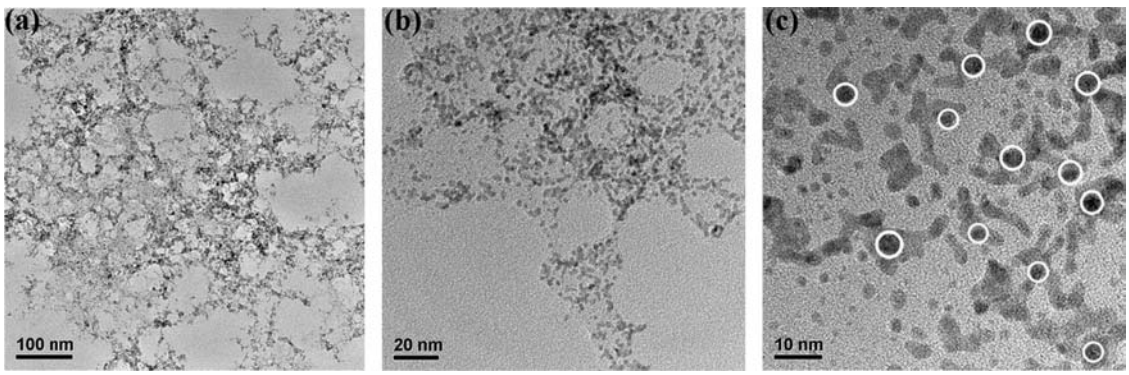

Fig. 1. (a, b) TEM and (c) HRTEM images of synthesized Pt-on-Pd/RGO (Pd center were denoted by white circles).

finally selected as the reaction medium in our experiment. Fig. 2a shows the UV–vis spectra of 1 mM TMB in the presence of 98 μM H_2O_2 before and after the addition of 5 μL Pt-on-Pd/RGO for 10 min at 30 °C. For comparison, the addition of RGO alone under the same conditions was also investigated. Generally, a UV–vis spectrometry technique allows to observe the charge transfer (CT) bands; the UV–vis spectra make possible to observe the electron transfer of one-electron associated with the TMB oxidation. In the experiments, two absorption peaks at 369 and 650 nm could be ascribed to the charge-transfer species derived from the one-electron oxidation of TMB [22] when Pt-on-Pd/RGO was present. Since the absorption at 369 nm was higher than that at 650 nm, the solution absorption at 369 nm was used to characterize the activities. It was obvious that Pt-on-Pd/RGO exhibited excellent peroxidase-like activity. Although RGO showed almost no activity under the same conditions, as a powerful 2D carbon material supporter and reductant, it played a key role in the synthesis of the Pt-on-Pd/RGO structure. Thus the observed peroxidase-like activity of Pt-on-Pd/RGO was attributed to the synergistic effect between Pt-on-Pd and RGO. Fig. 2b shows a photograph of the Pt-on-Pd/RGO in a solution containing 1 mM TMB and different concentrations of H_2O_2 (9.8, 0.98 and 0 μM) when the solution was incubated at 25 °C in pH 5.2 PBS for 20 min. A slight blue color (corresponding to the absorbance at 650 nm) could be observed even when the concentration of H_2O_2 was 0.98 μM, indicating that the system was very sensitive and that a qualitative analysis could be achieved simply using the naked eye. The color became darker with increase in the concentration of H_2O_2. In order to quantify the concentration of H_2O_2, the relationship between the absorption at 369 nm and the concentration of H_2O_2 was investigated. As shown in Fig. 3a, the absorption at 369 nm of this system increased with increasing H_2O_2 concentration. The detection limit for H_2O_2 could be calculated as 0.08 μM, which was comparable with or superior to that obtained from other methods [23,24]. Furthermore, the quantification limit for the proposed approach was found to be 0.3 μM H_2O_2. As shown in Fig. 3b, the calibration graph of the absorbance at 369 nm to H_2O_2 concentration was linear in the range from 0.3 to 130.7 μM. A correlation coefficient (R^2) of 0.998 could be obtained. Interestingly, in Fig. 3a, a small peak at 369 nm could also be observed in the absence of H_2O_2, indicating that the as-prepared Pt-on-Pd/RGO could even catalytically oxidize the TMB substrate using dissolved O_2 as a coreactant [25].

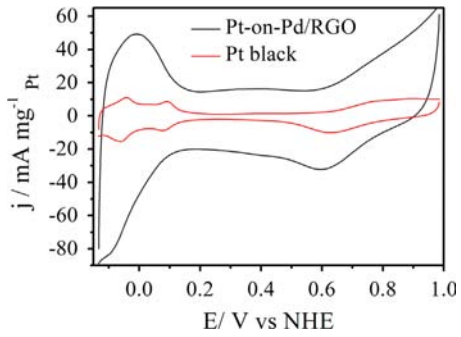

Fig. 4. CVs of Pt-on-Pd/RGO (outer cycle) and Pt black (inner cycle) in an aqueous solution containing 0.1 M H_2SO_4 at a scan rate of 50 mV s^{-1}.

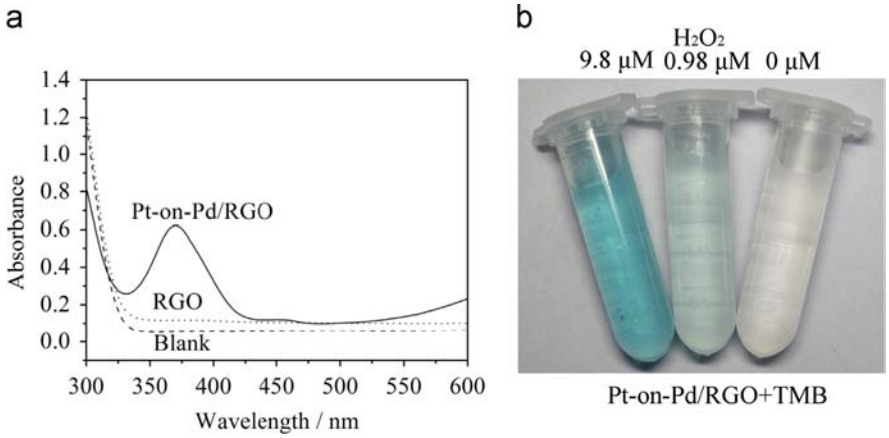

Fig. 2. (a) Typical absorption spectra of the 2 mM TMB (pH 5.2 PBS) and 98 μM H_2O_2 mixed solution before (dashed line) and after adding 5 μL Pt-on-Pd/RGO (solid line) or RGO (dotted line); all were incubated at 30 for 10 min. (b) Photograph of Pt Pt-on-Pd/RGO and TMB solution in the presence of different concentrations of H_2O_2.

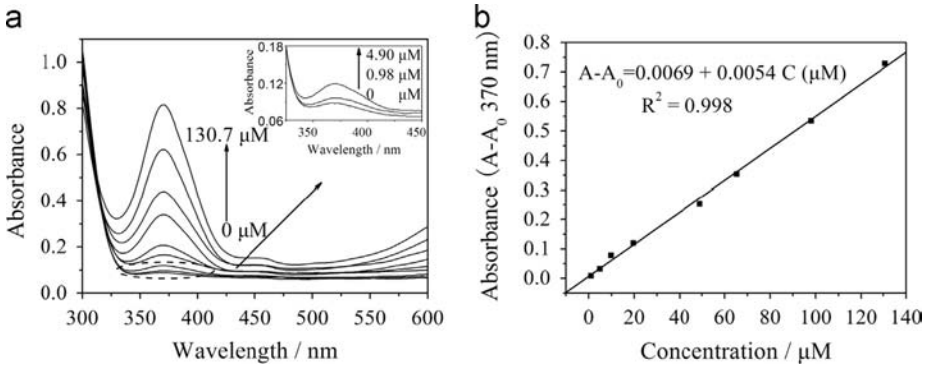

Fig. 3. (a) Absorption spectra of different concentrations of TMB–H_2O_2 in the presence of Pt-on-Pd/RGO. (b) The linear relationship between absorbance change and concentration of H_2O_2. Reaction conditions: pH 5.2 PBS and 2 mM TMB at 30 °C.

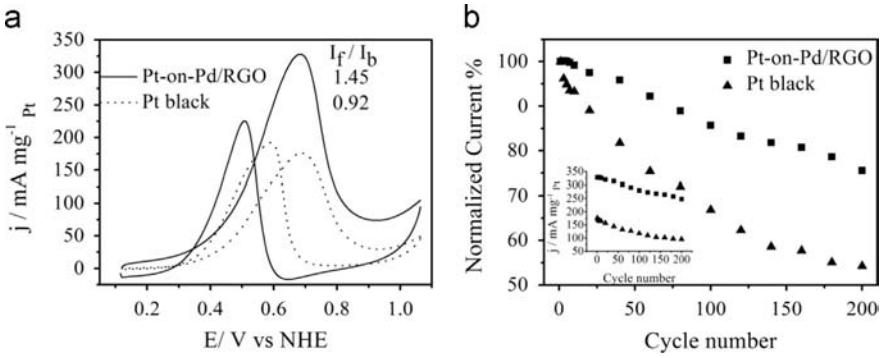

Fig. 5. (a) CVs of Pt-on-Pd/RGO (solid line) and commercial Pt (dashed line) black in 0.1 M H_2SO_4 contain 0.1 M CH_3OH with a scan rate of 50 mV s^{-1}. (b) Electro-catalytic cycling stability of Pt-on-Pd/RGO and Pt black in 0.5 M H_2SO_4 solution containing 0.1 M CH_3OH with 200 sequential scan. For convenience, only the 1st and 200th cycles were given.

3.3. Electro-oxidation of methanol

The catalytic property of Pt-on-Pd/RGO towards methanol electro-oxidation was carried out using a three-electrode system in 0.1 M H_2SO_4 and 0.1 M CH_3OH at 25 °C. For comparison, the catalytic performance of commercial Pt black was measured. All potentials in the cyclic voltammetry (CV) measurements were converted to the normal hydrogen electrode (NHE) values. Quantitative elemental analyses of Pt and Pd for the Pt-on-Pd/RGO were carried out using inductively coupled plasma mass spectroscopy. The CVs of Pt-on-Pd/RGO and Pt black in 0.1 M H_2SO_4 are presented in Fig. 4. The electrochemically active surface areas (ECSAs) could be estimated using the average of the area of hydrogen desorption and absorption. For Pt-on-Pd/RGO and Pt black, their ECSAs were found to be 64.9 and 17.9 $m^2\ mg_{Pt}^{-1}$, indicating that Pt-on-Pd/RGO had more active sites for catalytic application. As shown in Fig. 5a, the peak current density value (j_f) in a forward (positive) scan for Pt-on-Pd/RGO (328 mA mg_{Pt}^{-1}) was about 1.85 fold higher than that of Pt black (177 mA mg_{Pt}^{-1}). This result revealed the excellent electrochemical catalytic activity of the Pt-on-Pd/RGO toward methanol electro-oxidation, suggesting that the material has great potential in fuel cell applications. Furthermore, the ratio of the current density values in two sequential forward and backward (negative) sweeps (j_f/j_b) was 1.45 for Pt-on-Pd/RGO, which is much higher than the 0.92 obtained from Pt black. These results indicated that Pt-on-Pd/RGO has better tolerance to carbonaceous species accumulation [26,27]. In addition, after 200 cycles of sequential CV tests, j_f of Pt-on-Pd/RGO was 248 mA mg_{Pt}^{-1}, maintaining 75.5% of its initial activity, while for Pt black the values were only 95.6 mA mg_{Pt}^{-1} and 54.2%. These results revealed that the Pt-on-Pd/RGO was more durable and with higher electrocatalytic activity than the Pt black system in the electro-oxidation of methanol.

4. Conclusions

Pt-on-Pd/RGO hybrids were successfully synthesized using a facile hydrothermal method. Because of the synergistic effect between Pt-on-Pd and RGO, the synthesized Pt-on-Pd/RGO showed superior peroxidase-mimic activities in H_2O_2 reduction and TMB oxidation. An H_2O_2 sensing approach was developed using UV absorption with a linear range from 0.98 to 130.7 μM H_2O_2. In addition, the electrocatalytic oxidation of methanol property of the hybrid was investigated. The peak current density value j_f for Pt-on-Pd/RGO (328 mA mg_{Pt}^{-1}) was about 1.85 fold higher than that of Pt black (177 mA cm_{Pt}^{-2}) and more durable electro-catalytic activity was also obtained. For the first time, dual-functional Pt-on-Pd/RGO with peroxidase-mimic activities and an enhanced methanol electro-catalytic oxidation property was reported. It is believed that this novel composite will have more application in the areas of optical biosensors, electrochemical biosensors and fuel cells.

Acknowledgments

This research work was financially supported by the National Natural Science Foundation of China (21175112 and 21375112), which are gratefully acknowledged. Professor John Hodgkiss of The University of Hong Kong is thanked for his assistance with English.

References

[1] M. Campàs, B. Prieto-Simón, J.L. Marty, Semin. Cell Dev. Biol. 20 (2009) 3–9.
[2] A. Amine, H. Mohammadi, I. Bourais, G. Palleschi, Biosens. Bioelectron. 21 (2006) 1405–1423.
[3] L. Gao, J. Zhuang, L. Nie, J. Zhang, Y. Zhang, N. Gu, T. Wang, J. Feng, D. Yang, S. Perrett, Nat. Nanotechnol. 2 (2007) 577–583.
[4] M. Kajita, K. Hikosaka, M. Iitsuka, A. Kanayama, N. Toshima, Y. Miyamoto, Free Radic. Res. 41 (2007) 615–626.
[5] W. He, X. Wu, J. Liu, X. Hu, K. Zhang, S. Hou, W. Zhou, S. Xie, Chem. Mater. 22 (2010) 2988–2994.
[6] X. Sun, S. Guo, C.S. Chung, W. Zhu, S. Sun, Adv. Mater. 25 (2013) 132–136.
[7] K. Zhang, X. Hu, J. Liu, J.J. Yin, S. Hou, T. Wen, W. He, Y. Ji, Y. Guo, Q. Wang, Langmuir 27 (2011) 2796–2803.
[8] Y. Song, K. Qu, C. Zhao, J. Ren, X. Qu, Adv. Mater. 22 (2010) 2206–2210.
[9] Y. Tao, Y. Lin, Z. Huang, J. Ren, X. Qu, Adv. Mater. 25 (2013) 2594–2599.
[10] J. Chen, B. Lim, E.P. Lee, Y. Xia, Nano Today 4 (2009) 81–95.
[11] R. Service, Science 296 (2002) 1222.
[12] Y. Bing, H. Liu, L. Zhang, D. Ghosh, J. Zhang, Chem. Soc. Rev. 39 (2010) 2184–2202.
[13] W. Li, C. Liang, W. Zhou, J. Qiu, Z. Zhou, G. Sun, Q. Xin, J. Phys. Chem. B 107 (2003) 6292–6299.
[14] Y. Li, L. Tang, J. Li, Electrochem. Commun. 11 (2009) 846–849.
[15] N.S. Porter, H. Wu, Z. Quan, J. Fang, Acc. Chem. Res. 46 (2013) 1867–1877.
[16] F.F. Ren, H.W. Wang, C.Y. Zhai, M.S. Zhu, R.R. Yue, Y.K. Du, P. Yang, J.K. Xu W.S. Lu, ACS Appl. Mater. Interfaces 6 (2014) 3607–3614.
[17] S.S. Li, J.J. Lv, Y.Y. Hu, J.N. Zheng, J.R. Chen, A.J. Wang, J.J. Feng, J. Power Sources 262 (2014) 279–285.
[18] X.M. Chen, G.H. Wu, J.M. Chen, X. Chen, Z.X. Xie, X.R. Wang, J. Am. Chem. Soc. 133 (2011) 3693–3695.
[19] G.H. Wu, H. Huang, X.M. Chen, Z.X. Cai, Y.Q. Jiang, X. Chen, Electrochim. Acta 111 (2013) 779–783.
[20] Y. Zhu, S. Murali, M.D. Stoller, K. Ganesh, W. Cai, P.J. Ferreira, A. Pirkle R.M. Wallace, K.A. Cychosz, M. Thommes, Science 332 (2011) 1537–1541.
[21] S.J. Guo, S.J. Dong, E. Wang, ACS Nano 4 (2009) 547–555.
[22] P.D. Josephy, T. Eling, R.P. Mason, J. Biol. Chem. 257 (1982) 3669–3675.
[23] Y. Shi, P. Su, Y.Y. Wang, Y. Yang, Talanta 130 (2014) 259–264.
[24] H. Zheng, R.X. Su, Z. Gao, W. Qi, R.L. Huang, L.B. Wang, Z.M. He, Anal. Methods 6 (2014) 6352–6357.
[25] Y. Chen, H. Cao, W. Shi, H. Liu, Y. Huang, Chem. Commun. 49 (2013) 5013–5015.
[26] Y. Mu, H. Liang, J. Hu, L. Jiang, L. Wan, J. Phys. Chem. B 109 (2005) 22212–22216.
[27] A.X. Yin, X.Q. Min, Y.W. Zhang, C.H. Yan, J. Am. Chem. Soc. 133 (2011) 3816–3819.